Available online at www.sciencedirect.com

SciVerse ScienceDirect

Ceramics International 38 (2012) 2627–2632

CERAMICS INTERNATIONAL

www.elsevier.com/locate/ceramint

Review paper

Effect of high energy ball milling on compressibility and sintering behavior of alumina nanoparticles

A. Eskandari [a], M. Aminzare [a,*], Z. Razavi hesabi [a], S.H. Aboutalebi [b], S.K. Sadrnezhaad [c]

[a] Materials Engineering Department, Science and Research Branch, Islamic Azad University, Tehran, Iran
[b] Institute for Superconducting and Electronic Materials, ARC Centre for Electromaterials Science, University of Wollongong, NSW 2519 Wollongong, Australia
[c] Department of Materials Science and Engineering, Sharif University of Technology, Tehran, Iran

Received 3 September 2011; received in revised form 2 December 2011; accepted 6 December 2011
Available online 14 December 2011

Abstract

The effect of high-energy ball milling on the textural evolution of alumina nanopowders (compaction response, sinter-ability, grain growth and the degree of agglomeration) during post sintering process is studied. The applied pressure required for the breakage of the agglomerates (P_y) during milling was estimated and the key elements of compressibility (i.e. critical pressure (P_{cr}) and compressibility (b)) were calculated. Based on the results, the fracture point of the agglomerates decreased from 150 to 75 MPa with prolonged milling time from 3 to 60 min. Furthermore, the powders were formed by different shaping methods such as cold isostatic press (CIP) and uniaxial press (UP) to better illustrate the influence of green compact uniformity and powder deagglomeration on the densification behavior of nanopowders.

Keywords: A. Sintering; Nano alumina; Mechanical milling; Microstructure; Agglomeration

Contents

1. Introduction

Nanopowders, as a bridge between bulk materials and molecular or atomic structures, have attracted increasing attention due to their typically large surface area. The large surface area often dominates the properties of the powders and significantly enhances mechanical, chemical and physical properties of the material resulting in interesting and sometimes unexpected behavior of nanoparticles. For instance, larger surface area of nanopowders provides higher interaction surface area for catalysts, which in turn improves system efficiency [1–3]. Although larger surface area of nanopowders makes them promising candidates for many applications [4–6], the tendency to form agglomerates due to the considerable decrease in surface energy drastically affects their performance and expected properties.

There are three major microstructures that practically govern the processing and final properties of samples in fine-grained powders. These microstructures are namely primary crystallites, aggregates including some primary particles held together by neck areas, and agglomerates. Relatively weak attractive forces (i.e. van der Waals, capillary) are usually responsible for holding the primary crystallites and

* Corresponding author. Tel.: +98 912 5636521; fax: +98 21 7724 0291.
E-mail addresses: masoudaminzare@gmail.com, masoudaminzare@yahoo.com (M. Aminzare).

0272-8842/$36.00
doi:10.1016/j.ceramint.2011.12.012

aggregates within the structure of an agglomerate [7]. Therefore, in ultrafine and nano-grained powders, the existence of inter-agglomerate pores is noteworthy and usually leads to inevitable major problems in processing [8–12]. However, in most cases, better control of the pore geometry and an improvement of the mechanical properties of the porous structures are some of the important factors in improving the performance and reliability of these materials [13]. Therefore, considerable scientific research efforts have been conducted to find methods to break agglomerates and inter-agglomerates for direct and indirect application of nanopowders [7]. Due to the presence of agglomerates, compressibility of nanopowders decreases consequently leading to low green density of compacts which in turn results in rapid grain growth during sintering [14]. Higher sintering temperatures are often required to remove pores and obtain fully dense structures. As a result, significant grain growth occurs in the structure.

Other major points of concern in dry pressing process are how the granules and agglomerated powders flow and fill the forming die and how granules are deformed during the compaction process [15]. Higher fill density leads to higher green density and consequently higher sintered density. Moreover, inter-particle and particle–die interactions control powder compaction. It should be noted that the granules should be weak enough to be able to be deformed at low pressure and strong enough to better lead the rearrangement process.

Based on Hall–Petch equation [16], many investigations have been carried out to increase both hardness and strength [16–18]. High energy and high interface density are typically stored in fine and ultra fine structures. Dry pressing methods introduce micrometric inter-agglomerate pores and inter-crystalline pores into green bodies which subsequently degrades densification [19]. In contrast with dry pressing methods, sinter-forging (such as Hot Pressing SPS) or compaction of powders under extremely high pressures can be appropriate procedures to inhibit the growth of micrometric inter-agglomerate pores and inter-crystalline pores [9].

The present paper addresses the effects of the existence of agglomerates in nanopowders on the compaction and sinterability of shaped bodies. Furthermore, the effect of high energy ball milling on the textural evolution of alumina nanopowders in terms of the elimination of agglomerates is studied.

2. Materials and methods

Two types of alumina powder with mean particle size of 35 nm (Alfa Aesar) and 150 nm (Taimicron TM-DAR; Taimei Chemicals Co.) were used as starting materials. The morphology of powders was examined by scanning electron microscopy (XL30, Philips) using a 15 kV accelerating voltage. Powders were also examined on a transmission electron microscope (CM 200 FEG, Philips). The TEM samples were prepared by drying a droplet of the powder suspension on a holey carbon grid.

In order to break strong agglomerates, as-received nanopowders were mechanically milled in a high-energy ball mill (8000D mixer/mill, SPEX) with a ball-to-powder weight ratio of 10:1 for 3–60 min. To avoid contamination during the ball milling process, alumina vial and balls were used.

To investigate the effect of mechanical milling on compressibility, both as-received nanopowders and as-milled powders were uniaxially pressed in a cylindrical die (diameter: 10 mm) up to 700 MPa. To study the effect of the forming method on the densification of samples, the as-received powders were formed by cold isostatic press (CIP) at 150 MPa. Density of green samples was then measured using a volumetric method.

Green samples were then subjected to sintering at 1600 °C for 2 and 5 h. Water immersion technique was used to determine the density of the sintered pellet. Fractographic methods were utilized to study the microstructure of as-sintered samples.

3. Results and discussion

The bright filed TEM image presented at Fig. 1(a) indicates that the nanoparticles in the as-received alumina nanopowder

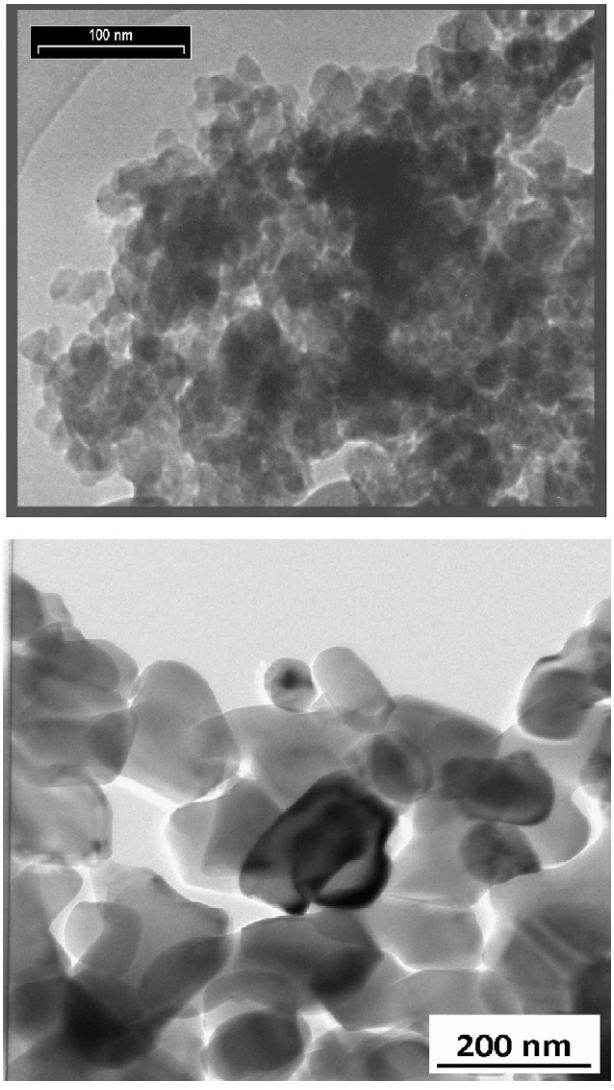

Fig. 1. TEM image of as-received Al_2O_3 (a) nano and (b) ultrafine powders.

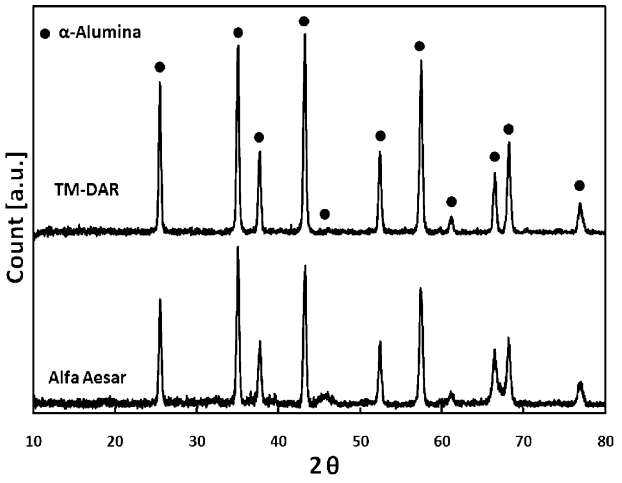

Fig. 2. XRD patterns of starting powders.

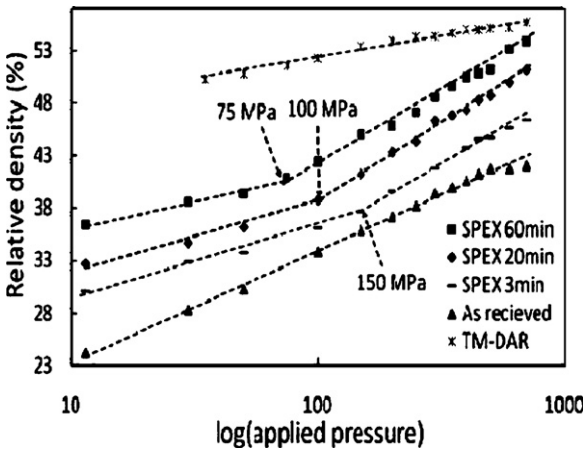

Fig. 4. Effect of mechanical milling on densification and agglomeration strength of Al_2O_3 nanopowder (arrows refer to the strength of the agglomerates).

are heavily agglomerated, which is consistent with the assumption that there are strong agglomerates in as-received nanopowders. Fig. 1(b) presents TEM micrograph of ultrafine Al_2O_3 powder demonstrating marginal agglomeration in the case of TM-DAR powders which are supposed to be agglomerate-free. Fig. 2 shows X-ray pattern of as-received powders. The prominent α alumina phase detected in XRD patterns clearly demonstrates that no phase transformation had occurred during the processing.

The compaction behavior of Al_2O_3 nanopowders is depicted in Fig. 3. Two regions can be identified in the curve. At lower pressure range (≤300 MPa), increasing the applied pressure gives rise to a rapid increase in the green density, while further increase in pressure is accompanied with just a marginal rise in density. For instance, upon increasing pressure from 11.5 to 300 MPa, green density of as received nanopowder reached 39 of theoretical density (TD) (15% increase in green density (from 24 to 39% TD)) however, further increase in pressure (≥300 MPa) led to only ∼4% increase in density. On the other hand, mechanically milled nanopowders exhibited better compressibility. For example, the green density of as-received

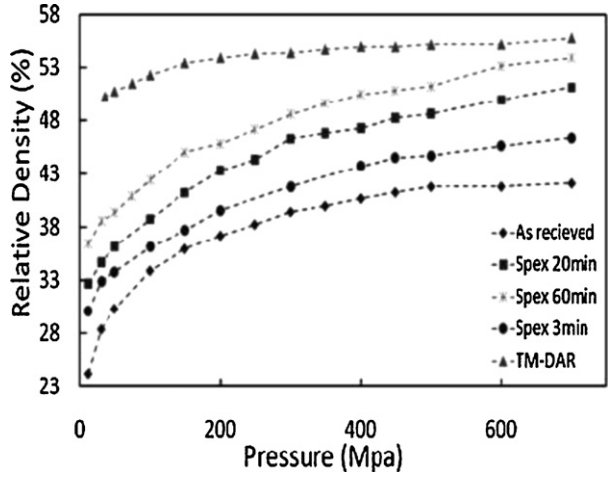

Fig. 3. Compaction behavior of as-received and mechanically milled Al_2O_3 nanopowder and free-agglomerated sub-micrometer powder.

nanopowder compacted at 700 MPa reached ∼42% TD while after just milling for 60 min the green density increased to 54% TD.

To better explain the results, it should be taken into account that the densification of powders is strongly influenced by powder characteristics such as average particle size, size distribution, shape, degree of agglomeration, and surface charges [20]. Typically, powders with smaller particle size exhibit a higher tendency to form agglomerates consequently leading to lower green density and less homogeneity of green compacts. The breakage of hard agglomerates due to mechanical milling and the decrease of agglomerate density in starting powder can result in higher green density of milled samples. Ferkel and Hellmig [10] reported improved compressibility of laser ablated synthesized ZrO_2 and Al_2O_3 nanopowder after mechanical milling.

Generally, there are different stages during the compaction of brittle powders. Sliding and rearrangement of particles/agglomerates, fragmentation of agglomerates, and elastic deformation of compacted powders are the typical stages during the compaction of brittle powders [21]. Relative density of compacted bodies as a function of applied pressure in logarithmic scale is illustrated in Fig. 4. It can be concluded that upon increasing the applied pressure, except for as-received and TM-DAR powders, a break point appears, which can be attributed to the strength of agglomerates. The change in the slope of the curve at break point implies that the second step of compaction is started. In other words, at the break point, the strong agglomerates and neck region between adjacent particles break down, and further increase in applied pressure results in higher green density and easy sliding of granules. Increasing the milling time from 3 to 60 min induces a sudden decrease in the agglomeration strength of nanopowders from 150 to 75 MPa, respectively. However, after ball-milling for 20 min, no extreme shift of the break point can be observed suggesting that the minimum agglomeration strength can be achieved after just 20 min ball milling period. Moreover, it is of interest to point out that no break point was observed for both as-received and TM-DAR compacts, which can be traced back to very

strong aggregates in the case of as-received powder and the agglomerate-free nature of TM-DAR (Fig. 1(b)).

To better illustrate the compaction behavior of nanopowders, key elements of compressibility were determined employing the following equation [22]:

$$\rho = b\,\mathrm{Ln}\left(\frac{P_{pr}}{P_{cr}}\right) + 1 \quad (1)$$

where ρ and P_{pr} are the density of green compact and compaction pressure, respectively. b and P_{cr} are ''the constant describing densification intensity of the compact powder'' and ''the critical compaction pressure at which the void free condition of a green compact is reached'', correspondingly.

Based on Eq. (1) and the slope of the curves (Fig. 4) after the break point (P_y), one can construe that an enhanced compressibility for the samples at the right hand side of the compaction curves can be observed. Our predictions given in Table 1, also confirm a higher b and a lower P_{cr} for applied pressures higher than P_y in contrast with the left hand side of the graphs. Analogously, Groot Zevert et al. [11] reported that after compaction of agglomerated particles at a pressure near P_y, the agglomerates are gradually fragmented, and their rearrangement occurs practically at lower pressures. As summarized in Table 1, while the value of b increases quickly at any point higher than P_y for all as-milled samples, the critical pressure (P_{cr}) decreases following the sudden increase in slope. These abrupt changes, however, confirm the improvement in the compaction behavior of samples.

Bazargan et al. [22] reported that higher b accompanied with a lower P_{cr}, can be attributed to a better compaction behavior of nanopowders. To the best of authors' knowledge, the verity of this idea is well established when the density of green compacts is taken into consideration. According to Table 1, 60-min milled samples have a lower b and higher P_{cr} in contrast with 3-min milled bodies before P_y; however, the sample exhibits much higher green density compared to 3 min milled samples. It is well known that longer ball milling time can lead to more effective elimination of soft agglomerates [10]; therefore, for 60-min milled powder pressed at a pressure just below P_y, from 30 to 50 MPa, the slope of compaction curve (compressibility) shows a lower value than the slope of the curve for 3-min milled sample due to the lower amount of soft agglomerates in 60-min milled sample. Further milling also resulted in increase in the surface area from 23.77 to 27.45 m^2/g from 3 to 60 min, respectively. The increase in surface area further proves the existence of fewer amounts of soft agglomerates in 60-min milled powder (Table 1). On the other hand, the lack of soft agglomerates in 60-min milled samples led to better flow-ability of powders which in turn resulted in higher green density compared the other samples pressed at the same pressure.

Table 1
Compressibility parameters of alumina nanopowders.

Sample	Condition	b	P_{cr} (MPa)	R^2	Surface area
As received	–	0.04592	1.744×10^8	0.9953	–
SPEX – 3 min	$P < P_y$	0.02895	3.675×10^{11}	0.9867	23.77
	$P > P_y$	0.05697	8.135×10^6	0.9938	
SPEX – 20 min	$P < P_y$	0.02775	4.41×10^{11}	0.9661	–
	$P > P_y$	0.06276	1.714×10^6	0.9953	
SPEX – 60 min	$P < P_y$	0.02277	1.556×10^{13}	0.9726	27.45
	$P > P_y$	0.05754	2.219×10^6	0.9937	
TM-DAR	–	0.01831	2.085×10^{13}	0.9797	–

The agglomerate-free nature of TM-DAR powder leads to higher flow-ability during the compaction process; therefore, higher green density values can be achieved. Because of this behavior, changing the applied pressure from 30 to 800 MPa causes only 6% increase in green density which results in the lowest b and highest P_{cr} values. The results obtained here are in agreement with Srdić et al. [23] They pressed two different synthesized nanopowders and plotted their green density–pressure plots. Compaction behavior for non-agglomerated powder was explained by a simple logarithmic relationship while the agglomerated one, in contrast, could be only explained by two logarithmic equations with a point of intersection [23]. Obviously, ball milling has a significant effect on agglomerated powders leading to better compaction response. Therefore, higher green density and better sinterability would be achieved.

The fractional density of starting alumina nanopowders with the mean particle size of 35 nm, sintered at 1600 °C for 2 and 5 h, as a function of applied pressure is shown on Fig. 5. The relative fired density of as-received powder compacted samples at 1600 °C for 2 h is at best 70%; while the highest density

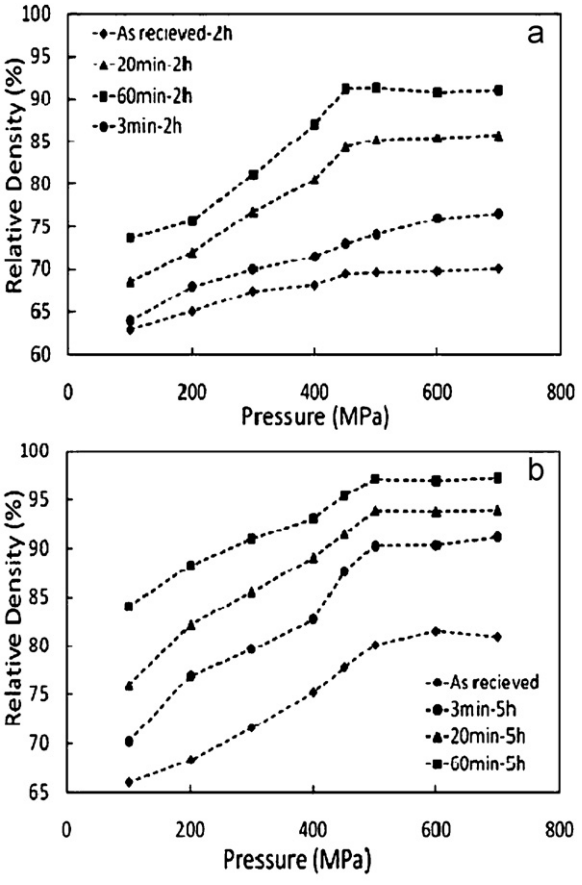

Fig. 5. Fractional density of nano alumina compacts after (a) 2 h and (b) 5 h sintering at 1600 °C.

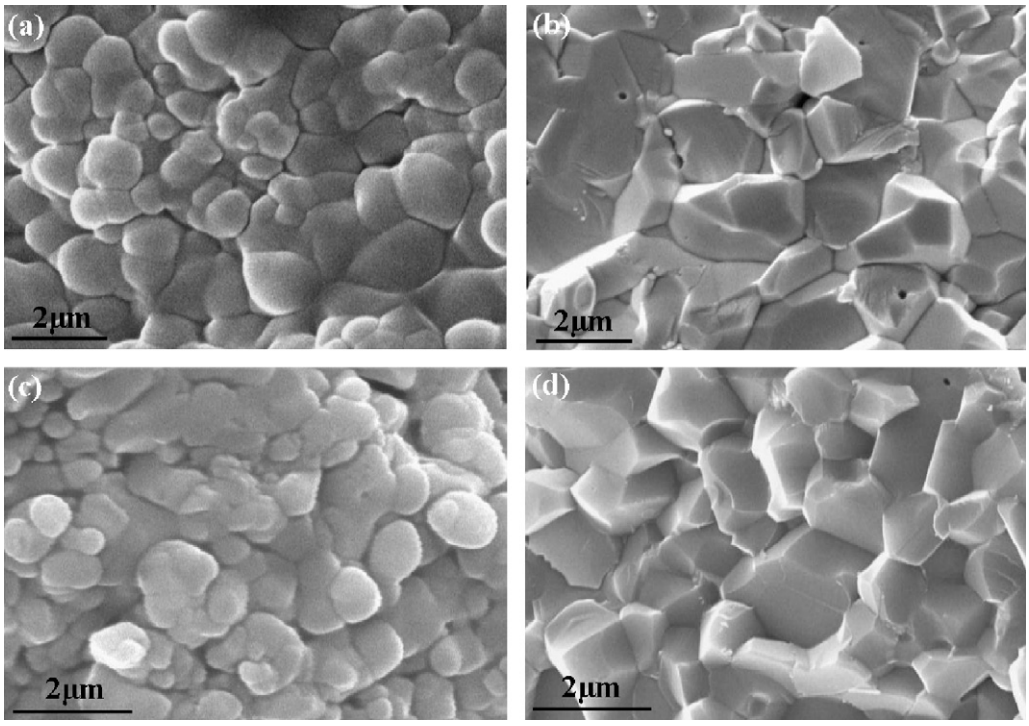

Fig. 6. SEM micrographs of fracture surfaces of alumina compacts at 700 MPa and sintered at 1600 °C. Powders were milled for 3 min and sintered for 2 h (a) and 5 h (b). 60 min milled samples and sintered for 2 h (c) and 5 h (d) are displayed.

(89.5%) was achieved for the sample sintered for 2 h and milled for 60 min. The fractional density of 3 min milled samples increased rapidly upon increasing the compaction pressure below 500 MPa, whereas the fractional density became almost constant after 500 MPa. 20 and 60-min milled powders also exhibited the same densification trend. On the other hand, fractional densities of 20, 60-min milled powder compacts are almost constant upon applying pressures above 600 MPa. Higher dwelling time (5 h) also resulted in higher fractional density (Fig. 5(b)). Upon increasing the sintering time from 2 to 5 h, fractional density of as-received compact powder increased ∼10% at 700 MPa. Furthermore, by increasing the milling time up to 60 min, fractional densities of compact samples were enhanced. Li and Ye [24] reported a relative density of over 95% for alumina compacts fabricated from nanopowders with a mean particle size of 48 nm pressed at 1420 MPa and sintered at 1500 °C for 5 h. Here, we achieved a maximum value of 97.2% TD at only 500 MPa by merely milling the powders for 60 min. It is claimed that [10] by modifying the nanopowders, sintering activity and green densities of compact samples can be improved. In fact, deagglomeration of ceramic nano particles (e.g. by high-energy mechanical milling, chemical method) reduces the neck area among adjacent particles and results in better sintering behavior. Krell et al. [20,25] have also reported that the important factors to achieve sub-micrometer structure bodies are not only selecting the fine raw materials but also processing them to avoid strong agglomerates. They have concluded that employing aggregate-free powder as raw material results in less sintering temperature and consequently less grain growth. Likewise, the densification trend for 5 h sintered pellets after 3, 20 and 60 min milling is approximately the same. In fact, after applying 500 MPa, relative densities tend to come toward a constant value and even show a slight decrease. This trend can be attributed to the grain growth and release of residual stress, which results in a directional force applied on the grain during the compaction process.

The SEM micrographs of as-sintered alumina from starting nanoparticle (35 nm) are shown in Fig. 6. SEM was used to assess the size of as-sintered samples. 3-min milling followed by sintering for 2 h resulted in grains with a lateral size dominantly in the order of 0.75 μm. Increasing the milling time to 60 min led to finer microstructure consisting of grains with a diameter of less than 0.5 μm.

Regarding the case of longer sintering time (5 h), grain growth is more enhanced. In fact, the average grain size of 3-min milled powder was almost 2 μm. It is clear that increasing the milling time does not result in any considerable difference in grain size of Al_2O_3 sintered pellets.

The differences between green and sintered densities according to forming methods are listed in Table 2. For agglomerated alumina nano powder, compact density is about 35.6% (at 150 MPa); however, cold pressing isostatically yields a density of 39.4% TD. Hence, the final density of the samples prepared employing CIP method was also higher than the ones prepared employing uniaxial pressing. The reason lies in the fact that employing cold isostatic press can lead to both narrower pore size distribution and smaller pore size; therefore, the uniform structure of green compacts prepared by CIP method provides higher fired density in comparison with uniaxially pressed ones. Razavi Hesabi et al. [19] have also reported that CIP samples of alumina powder exhibited smaller and narrower pore size distribution than uniaxially pressed

Table 2
Green and final densities of alumina modified powders with different shaping methods.

Forming method	Sample	Relative green density (%)	Relative sintered density (2 h, %)	Relative sintered density (5 h, %)
CIP	As received	39.4	73.6	79.5
UP	As received	35.6	63.7	68.3
TM-DAR (CIP)	As received	57.5	97.01 (at 1400 °C, without soaking time)	–

bodies. Krell et al. [20,25] indicated that alumina bodies formed by CIP reach their approximate theoretical density 150 °C lower than the samples shaped by uniaxial press. In addition, TM-DAR alumina samples showed good compaction and densification properties (more than 57% green density and 97% fired density without any soaking time at 1400 °C) confirming the agglomerate-free nature of TM-DAR powder.

4. Conclusion

Compaction response of alumina nano powders (35 nm) containing hard agglomerates with respect to agglomerate-free alumina nanopowder was investigated. It was demonstrated that deagglomerating nano powders employing high-energy ball milling results in higher green and sintered density. Further milling time shifted the break point. CIP was employed to compare the effect of forming method on the densification behavior of as-received nanopowders. It was concluded that isostatic pressing is preferable than uniaxial press approach at the same pressure due to a ∼10% increase in density after 2 h of sintering. In addition, higher fractional density and grain growth was obtained by longer sintering time (5 h).

References

[1] J. Zhu, M. Zach, Nanostructured materials for photocatalytic hydrogen production, Curr. Opin. Colloid Interface Sci. 14 (2009) 260–269.
[2] M. Watanabe, H. Yamashita, X. Chen, J. Yamanaka, M. Kotobuki, H. Suzuki, H. Uchida, Nano-sized Ni particles on hollow alumina ball catalysts for hydrogen production, Appl. Catal. B: Environ. 71 (2007) 237–245.
[3] S.A. Hassanzadeh-Tabrizi, M. Mazaheri, M. Aminzare, S.K. Sadrnezhaad, Reverse precipitation synthesis and characterization of CeO_2 nanopowder, J. Alloys Compd. 491 (2010) 499–502.
[4] E.S. Kawasaki, A. Player, Nanotechnology, nanomedicine, and the development of new effective therapies for cancer, Nanomed. Nanotechnol. Biol. Med. 1 (2005) 101–109.
[5] L. Tsakalakos, Nanostructures for photovoltaics, Mater. Sci. Eng. R 62 (2008) 175–189.
[6] S.R. Kamboj, B. Sekhon, Inorganic nanomedicine. Part 2, Nanomed. Nanotechnol. Biol. Med. 6 (2010) 612–618.
[7] V.T. Zaspalis, E.S. Kikkinides, M. Kolenbrander, R. Mauczok, Method for the morphological characterization of powder raw materials for the manufacturing of ceramics, J. Mater. Process. Technol. 142 (2003) 267–274.
[8] M. Aminzare, F. Golestani-fard, O. Guillon, M. Mazaheri, H.R. Rezaie, Sintering behavior of an ultrafine alumina powder shaped by pressure filtration and dry pressing, Mater. Sci. Eng. A 527 (2010) 3807–3812.
[9] P. Bowen, C. Carry, From powders to sintered pieces: forming, transformations and sintering of nanostructured ceramic oxides, Powder Technol. 128 (2002) 248–255.
[10] H. Ferkel, R.J. Hellmig, Effect of nanopowder deaglomeration on the densities of nanocrystalline ceramic green bodies and their sintering behavior, Nanostruct. Mater. 11 (1999) 617–622.
[11] W.F.M. Groot Zevert, A.J.A. Winnubst, G.S.A.M. Theunissen, A.J. Burggraaf, Powder preparation and compaction behaviour of fine-grained Y-TZP, J. Mater. Sci. 25 (1990) 3449–3455.
[12] R. Vaûen, D. StoÈver, Processing and properties of nanophase ceramics, J. Mater. Process. Technol. 92–93 (1999) 77–84.
[13] A. Dakskobler, A. Kocjan, T. Kosmac, Porous alumina ceramics prepared by the hydrolysis-assisted solidification method, J. Am. Ceram. Soc. 94 (2011) 1374–1379.
[14] J. Ahn, M. Huh, J. Park, Effect of green density on subsequent densification and grain growth of nanophase SnO_2 powder during isothermal sintering, Nanostruct. Mater. 8 (1997) 637–643.
[15] K.G. Ewsuk, J.G. Arguello, D.N. Bencoe, D.T. Ellerby, S.J. Glass, D.H. Zeuch, J. Anderson, Characterizing powders for dry pressing, sintering, Am. Ceram. Soc. Bull. 82 (2002) 41–47.
[16] M.A. Meyers, A. Mishra, D.J. Benson, Mechanical properties of nanocrystalline materials, Prog. Mater. Sci. 51 (2006) 427–556.
[17] M. Aminzare, M. Mazaheri, F. Golestani-fard, H.R. Rezaie, R. Ejeian, Sintering behavior of nano alumina powder shaped by pressure filtration, Ceram. Int. 37 (2011) 9–14.
[18] K.A. Padmanabhan, Mechanical properties of nanostructured materials, Mater. Sci. Eng. A 304–306 (2001) 200–205.
[19] Z. Razavi Hesabi, M. Haghighatzadeh, M. Mazaheri, D. Galusek, S.K. Sadrnezhaad, Suppression of grain growth in sub-micrometer alumina via two-step sintering method, J. Eur. Ceram. Soc. 29 (2009) 1371–1377.
[20] A. Krell, P. Blank, The influence of shaping method on the grain size dependence of strength in dense submicrometre alumina, J. Eur. Ceram. Soc. 16 (1996) 1189–1200.
[21] K.G. Ewsuk, J.G. Arguello, D.N. Bencoe, D.T. Ellerby, S.J. Glass, D.H. Zeuch, Characterizing powders for dry pressing, sintering, Am. Ceram. Soc. Bull. 82 (2002) 41–47.
[22] A.M. Bazargan, M. Naghavi, M. Mazaheri, S.K. Sadrnezhaad, Simultaneous synthesis and single-step sintering of lead magnesium niobate ceramic using mixed nanopowders, Ceram. Int. 35 (2009) 1139–1144.
[23] V. Srdić, M. Winterer, H. Hahn, Sintering behavior of nanocrystalline zirconia doped with alumina prepared by chemical vapor synthesis, J. Am. Ceram. Soc. 83 (2000) 1853–1860.
[24] J. Li, Y. Ye, Densification and grain growth of Al_2O_3 nanoceramics during pressureless sintering, J. Am. Ceram. Soc. 89 (2006) 139–143.
[25] A. Krell, P. Blank, H. Ma, T. Hutzler, M. Nebelung, Processing of high-density submicrometer Al_2O_3 for new applications, J. Am. Ceram. Soc. 86 (2003) 546–553.